

# Finite Element Analysis and Design of Test Setup for Determination of Transfer Length in BFRP Prestressed Concrete Beams

Prashant Motwani, Shruti Dhruw and Arghadeep Laskar\*

This work is a vital step in enhancing the potential use of a newly developed organic basalt fibre reinforced polymer (BFRP) bars for prestressed concrete applications. In the present study, a test setup has been designed using finite element analysis (FEA) and the various steps of prestressing such as initial prestress, effective prestress and the time dependent effects have been appropriately simulated in the finite element (FE) model. The configuration details of the test setup, such as the size and orientation of the sections and the location of the stiffener plates have been thoroughly investigated. A robust design of the setup has been established based on the FEA results. Subsequently, the FE model has been utilized to predict the transfer stage parameters for concrete beams prestressed using BFRP bars. The transfer length has been predicted from the FEA results to be  $24d_b$  and  $26d_b$  (where,  $d_b$  is the diameter of bar) when measured using the BFRP bar strains and the concrete strains, respectively. An end slip of 0.3mm has been obtained after the prestressing of concrete beams. The designed test setup will be later fabricated and utilized to perform experiments under laboratory-controlled conditions.

## Introduction

Pre-stressed concrete (PC) members degrade rapidly when the steel strands are subjected to corrosion thereby decreasing the lifespan of the PC structures. Two major bridge collapses in the past; the failure of the viaduct “S. Stefano” in Italy in the year 1999 [1] and Charlotte’s Motor Speedway footbridge in the USA in the year 2000 [2] has been related to the corrosion of the prestressing steel strands. The maintenance of steel (to prevent it from corrosion) and replacement of the assets (which are affected by corrosion) in a short span of time has become a major concern for an economy. Therefore, it is imperative that corrosion is dealt with utmost priority so that the full effect of the growth may be felt in the infrastructure industry. The concern for durability and prolonged service life of PC structures is rapidly gaining importance with ACI Committee releasing a report ACI 440R.04 [3] in the year 2004 for replacing steel strands in prestressed concrete (PC) members with fiber reinforced polymer (FRP) bars. In addition to the corrosion related issues, the loss of prestress force which can go upto 24% is another major concern for

steel PC members [4]. Due to the above reasons there has been considerable research in the past to replace the steel strands in PC members with FRP bars [5-8]. The most widely accepted materials used in the fibers of FRPs are aramid and carbon. However, both these materials have their own demerits. The sensitivity of aramid FRP to sunlight and UV environment [9] and the high electrical conductivity of carbon FRP [10] are the major drawbacks of these materials.

Basalt fiber reinforced polymer (BFRP) bar is a newly developed organic polymer with high resistance to UV exposure, low thermal and electrical conductivity and high resistance to chemical attack [11]. They have a great potential application as a composite material. Overall, the manufacturing process of BFRP is similar to glass FRP, but with significantly lower energy consumed during the manufacturing process. Using a natural volcanic basalt rock as raw material, basalt fibers are produced by charging raw materials into a furnace where they are melted at 1450 °C to 1500 °C. The molten material is then forced through platinum/rhodium crucible bushings to convert it into fibers. This technology, named continuous spinning, can offer the reinforcement material in the form of chopped or continuous fibers that can be utilized as raw material in various industries like, infrastructure, textile, automobile, etc. In addition to the ability to be easily processed using conventional methods and equipment, the basalt fibers do not contain any other additives in the entire production process, which makes it economical compared to other FRP

Civil Engineering Department, IIT Bombay, Powai, Mumbai, Maharashtra 400076, India

\*Corresponding author: E-mail: laskar@civil.iitb.ac.in

DOI: 10.5185/amlett.2021.091660

[11]. Abed *et. al.*, [12-14] performed extensive experimental and finite element investigation on the flexural and compression behaviour and serviceability performance of BFRP reinforced concrete (RC) members. Although studies related to the behaviour of BFRP bars as a reinforcing material is available for normal and harsh environment [15,16], there is limited research available on the behaviour of BFRP bars when used as a prestressing element. Systematic research conducted by Wu *et. al.*, [17] have reported high rupture strength (950 MPa to 2000 MPa) and a relatively low elastic modulus, ranging (45 GPa to 55 GPa) for BFRP bars. This indicates that the strength of BFRP bars is comparable to steel prestressing strands, while having an elastic modulus four times smaller and weight four times lighter. Thus, BFRP bars can be an alternative to steel prestressing strands for PC applications. The mechanical properties of the BFRP bars and other component parts of the test setup utilized in the present simulation are shown in **Table 1**.

The present study aims to establish a comprehensive design of a manufacturing and testing facility to cast and prestress concrete members with BFRP bars as prestressing element using fundamentals of engineering mechanics and utilize finite element analysis (FEA) technique to further optimize the design based on the maximum elastic deformation and Von Mises failure criteria. Furthermore, critical service stage parameters like immediate and long-term transfer length and end slips in BFRP prestressed concrete member have been predicted based on the FEA results before the actual fabrication of the test set-up.

### Test setup

The test setup has been designed to fabricate and prestress two identical concrete beams with subsequent measurement of critical service stage parameters such as transfer length and end slips. The frame of the test-setup has been designed as a self-equilibrating steel frame and the forces acting on each component part of the framework are balanced by formulating a box-shaped configuration. The force

equilibrium has been ensured by balancing the forces F1 and F2, as shown in **Fig. 1**.

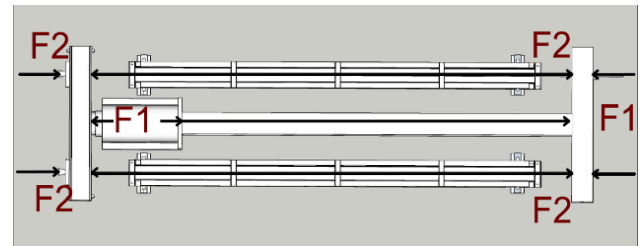


**Fig. 1.** Schematic Depiction of the Framework.

The net torque on the system due to forces F1 and F2 have been avoided to achieve the three-dimensional (3D) equilibrium of the test framework. This has been achieved by maintaining the same height of the centre of gravity for each component part and thereby ensuring that the torque is balanced between the force systems F1 and F2. The complete details of the manufacturing facility along with the specifics of the individual parts of the frame can be found in the disclosure filed with the Indian Patent Office [27].

### Finite element analysis

A three-dimensional finite element (FE) model of the test setup has been developed using ABAQUS to generate the proof of concept and facilitate in further refinement of the setup design. The FE modelling process meticulously reflects all the experimental conditions initiating with the tensioning operation and followed by the stress transfer and the time dependent behaviour. The configuration details of the test setup shown in **Fig. 2** have been designed by conducting a parametric study on the developed model and the effect of several parameters like the size and orientation of the sections and location of the stiffener plates on the overall performance of the test setup have been thoroughly investigated.

**Table 1.** Material Properties Utilized in Finite Element Model.

Parameter	BFRP	Concrete	Structural Steel	Anchors	
				Barrel	Wedge
Tensile Strength, MPa [18] [19] [20] [21]	920	3.20	410	1580	1975
Yield Stress, MPa [20][21]	N.A.	N.A.	250	1366	1896
Ultimate Compressive Strength, MPa [18] [22]	460	32	*	*	*
Longitudinal Modulus, GPa [18] [19] [21] [20]	37	25.78	200	200	200
Transverse Modulus, GPa [22]	4.17	N.A.	200	200	200
Ultimate Tensile Strain [18] [19] [21] [20]	0.01703	0.0002	0.23	0.13	0.13
Inter-laminar Shear Strength, MPa [22]	72.4	N.A.	N.A.	N.A.	N.A.
Peak Bond Stress, MPa [23]		26.71	N.A.	N.A.	N.A.
Slip at Peak Bond Stress, mm [23]		0.30	N.A.	N.A.	N.A.
Transverse Shear Strength, MPa [24]	315.3	*	*	*	*
Major Poisson's Ratio [25][21]	0.284	0.15	0.30	0.30	0.30
Minor Poisson's Ratio [25]	0.054		0.30	0.30	0.30
In-Plane Shear Modulus, GPa [26]	7.20	*	*	*	*
Transverse Shear Modulus, GPa [26]	1.98	*	*	*	*

Note: \* indicates that the information is not available.

### Analysis steps

The present analysis has been performed in six different steps. The first step represents the pretensioning operation in which the distribution of the stresses along the length of the 8 mm diameter prestressing BFRP bar remains constant and equal to the initial prestress. This has been achieved by defining a pre-determined displacement to the spandrel beam in order to stretch the BFRP bar to an initial prestress value of  $0.40f_{pu}$  (where,  $f_{pu}$  is the ultimate strength of the bars). The upper limit of the initial prestress has been selected to be within the maximum permissible initial prestress limit ( $0.55f_{pu}$ ) as per ACI 440.4R [3] guidelines.

The second analysis step represents the casting of concrete beams and the release of prestressing bar. The bond stress-slip relationship between the BFRP bar and the surrounding concrete has been defined in this step to simulate prestressing of the concrete beams. The release of the BFRP bar has been implemented by releasing the displacement given to the spandrel beam in the previous step. Since the strains in the BFRP bar are within the elastic limit and the bars are locked at both ends using wedge anchors, the movement of the spandrel beam back to its original position is restricted due to the bond between the prestressing BFRP bar and concrete. This results in the transfer of prestress from the BFRP bar to the concrete beam. The third to sixth steps of the analysis represent the shrinkage and creep of concrete. The time dependent behaviour of concrete has been simulated in ABAQUS by varying the modulus of elasticity of concrete in the developed FE model of the concrete beam. The mean compressive strength of concrete after  $t$  days, denoted as  $f_{cm}(t)$ , and the variation of Young's modulus of concrete with time, denoted as  $E_{cm}(t)$ , has been estimated using Eurocode-2 [28]. A field variable (FV) has been defined in the ABAQUS CAE which considers the variation in the elastic modulus with the ageing of concrete and simulates the changed behavior of concrete at different ages due to shrinkage and creep. Moreover, a much more detailed and comprehensive explanation of the procedure to simulate the time dependent behaviour of concrete in ABQUS has been presented in a previous study on influence of end slippage on transfer length of prestressing strands [29].

### Input parameters

The constitutive relationship for materials, contact behavior, constraints and appropriate boundary conditions such as displacement and/or force boundary conditions have been defined as the required input to develop the FE model of the test setup. The prestressing element (BFRP) has been modelled as a linear transversely isotropic material. The material properties required to simulate the mechanical behavior of the BFRP bars are shown in **Table 1**. The elastic-plastic response of concrete has been simulated using the concrete damage plasticity (CDP) model. The generalized compressive stress-strain relationship of concrete reported by Mander *et. al.* [18]

which relates the uniaxial compressive stress to uniaxial compressive strain has been utilized as an input for the CDP model. The default values of the dilation angle ( $\Psi$ ), eccentricity ( $e$ ), ratio of biaxial and uniaxial compressive yield stress ( $\zeta$ ), stress variant ratio ( $k$ ) and viscosity parameter ( $\mu$ ) available in the ABAQUS user manual as  $35^\circ$ , 0.1, 1.16, 0.67 and 0.01, respectively have been selected to define the CDP model. The deterioration of the material stiffness follows an isotropic behaviour in the CDP model and the material compression stiffness damage variable ( $d_c$ ) has been defined in the numerical model using **Eq.1**.

$$d_c = 0 \quad ; \quad \varepsilon_c \leq \varepsilon_{cm}$$

$$= 1 - \frac{\sigma_c}{\sigma_{cm}} \quad ; \quad \varepsilon_c > \varepsilon_{cm}$$
Eq. 1

In **Eq. 1**,  $\varepsilon_{cm}$  is the maximum strain in concrete corresponding to maximum compressive stress ( $\sigma_{cm}$ ). The inelastic strain values ( $\varepsilon_c^{in}$ ) of concrete have been obtained from the strain values in concrete ( $\varepsilon_c$ ) corresponding to compressive stresses ( $\sigma_c$ ), by using **Eqs. 2** and **3**. The stress and the corresponding inelastic strain values have been thereafter provided as the input to the CDP model to define the constitutive properties of concrete.

$$\varepsilon_c^{in} = \varepsilon_c - \varepsilon^{el}$$
Eq. 2

$$\varepsilon^{el} = \frac{\sigma_c}{E_c}$$
Eq. 3

The concrete damage states in the FE model have been identified through the equivalent plastic strain in compression ( $\varepsilon_c^{pl}$ ). It has been ensured that the values of  $\varepsilon_c^{pl}$  calculated using **Eq. 4** is always greater than  $\varepsilon_c^{in}$  in order to ensure convergence of the nonlinear analysis algorithm. Hence, the decreasing values of  $\varepsilon_c^{pl}$  (if any) have been manually eliminated from the constitutive model to ensure that  $\varepsilon_c^{pl}$  is always greater than  $\varepsilon_c^{in}$  throughout the analysis.

$$\bar{\varepsilon}_c^{pl} = \bar{\varepsilon}_c^{in} - \frac{d_c}{1-d_c} \frac{\sigma_c}{E_c}$$
Eq. 4

A quad-linear material model proposed by Yun and Gardner [21] for FE-410 steel has been utilized to model the constitutive relationship for the stiffener plates, the back-supporting beam, the mid-supporting beam and the spandrel beam of the test setup. The model accurately represents the elastic, yield plateau and strain hardening properties typically associated with hot-rolled steel sections. Standard industrial anchors utilized in the experimental investigation on BFRP bars conducted by Motwani *et. al.*, [19] have been modelled to pretension the BFRP bars in the test setup. The yield and ultimate tensile strengths of the barrel of the anchors have been taken as 1366 MPa and 1580 MPa respectively. The yield and ultimate tensile strengths of the wedges of the anchors have been taken as 1896 MPa and 1975 MPa, respectively. The

Young's Modulus of elasticity, the Poisson's ratio and the ultimate tensile strain of the barrel and the wedges of the anchors have been defined as 200 GPa, 0.3 and 13%, respectively. Thus, bilinear elastic-plastic models have been used to model the barrel and wedge assembly of the anchors.

Several contact definitions have been utilized to model the contact behavior between the various interaction surfaces. A frictionless model has been selected to define the contact between the two ISMB 450 sections and their connection with the stiffener plates. The interaction between the prestressing bar and the surrounding concrete has been simulated by defining the tangential and the cohesive behavior of the interaction surfaces between the two materials. The tangential behavior has been implemented in the numerical model by defining a penalty friction of 0.55 based on the recommendations of the AASHTO LFRD [30].

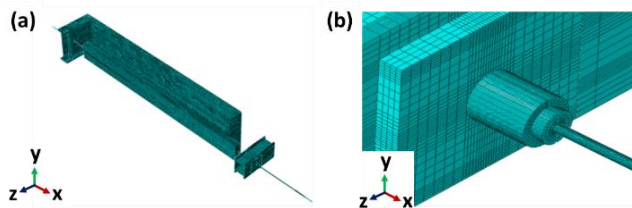


Fig. 2. Finite Element Model (a) Assembly and (b) Meshing.

The cohesive surface-based approach has been utilized to define the bond-stress v/s slip relationship through the typically known linear traction-separation model available in ABAQUS library. The stiffness coefficient necessary to define the traction-separation matrix has been obtained by dividing the peak bond-stress and the corresponding slip at peak bond-stress reported in **Table 1**. The stiffness along the normal direction has been taken as 100 times the stiffness along the tangential direction. A comprehensive description of the formulation of the linear traction-separation model used for the simulation of prestressed concrete members in ABAQUS can be found in a previous study on FEA of pretensioned bridge girders [32]. It is to be noted that the damage evolution (cohesion softening) of the bond can be simulated by defining the damage variable corresponding to the plastic slip values. However, the scope of the present simulation was to evaluate the transfer stage parameters and a bond-damage is unlikely to occur during prestress transfer. Moreover, since, the traction-separation stiffness matrix is independent of the Young's modulus of concrete and utilizes only peak bond stress and corresponding slip, the change in bond characteristics with aging of concrete has not been considered in the present study.

Due to the frame symmetry, half-model of the test set-up has been developed with appropriate boundary conditions applied on the plane of symmetry. An X displacement (refer **Fig. 2**) of 31 mm has been applied to the central portion of the spandrel beam

in order to stretch the BFRP bars to 40% of their ultimate strength. The displacement magnitude has been selected based on the expected elongation of the prestressing BFRP bar with due consideration of the anchor slips.

## Results and discussion

### Initial prestress and optimization results

The primary purpose for the optimization of the component parts of the test setup was to avoid any damage or development of plastic strains in the test set-up during the initial prestressing stage. Thus, the FEA results after the initial prestress analysis step have been utilized to ensure that the test set-up has enough reserved strength during the prestressing operation.

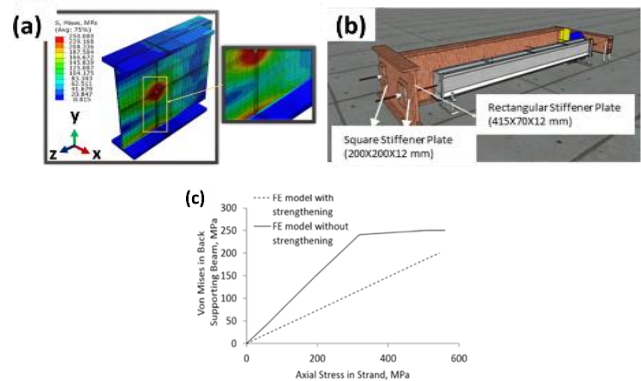
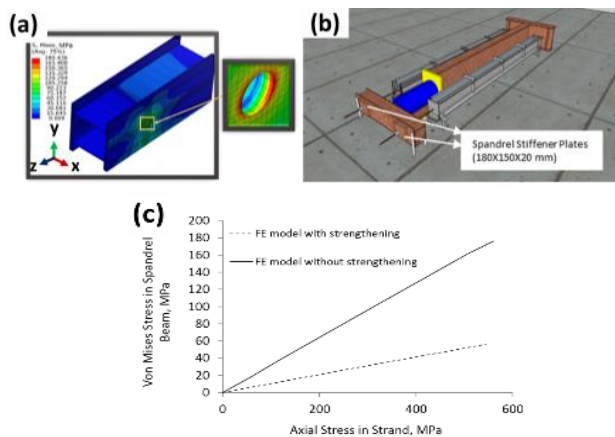


Fig. 3. Strengthening of Back Supporting I-beam (a) Von Mises Stress Distribution, (b) Location of additional Stiffeners, and (c) Improved FEA Results.

The stress distribution in the back supporting I-beam obtained at the end of the first analysis step (**Fig. 3**) has been observed to exceed the Von Mises yield criteria defined in the FE model. The location of the plastic strains was primarily concentrated at the hole location and at the top and bottom flange portions of the back supporting I-beam (**Fig. 3(a)**). Thus, the back supporting I-beam has been strengthened by adding two rectangular stiffener plates (dimensions 415 mm X 70 mm X 12 mm) extending from the top flange to the bottom flange. Two square stiffener plates of dimensions 200 mm X 200 mm X 12 mm have also been added at the hole locations of the back supporting I-beam (**Fig. 3(b)**). The maximum Von Mises stress obtained from the stiffened and unstiffened FE models have been plotted with the increase of the axial stress in the BFRP bar as shown in **Fig. 3(c)**. It can be observed that the Von Mises stress has reduced significantly and a factor of safety (FOS) of 1.25 has been ensured at the critical location of the back supporting I-beam.

The stresses in the spandrel beam have been observed to satisfy the Von Mises yield criteria defined in the FE model (**Fig. 4(a)**). However, two stiffener plates of dimensions 180 mm X 150 mm X 20 mm have been added

at the hole location of the spandrel beam (**Fig. 4(b)**) in order to increase the FOS and reduce the maximum stress value. The variation of the Von Mises stress at the critical location of the spandrel beam with the increase of axial stress in the BFRP bar has been plotted as shown in **Fig. 4(c)**. The addition of the stiffener plate results in the reduction of the Von Mises stress in the spandrel beams and a FOS of 3.0 has been ensured at the end of initial prestress step. The higher FOS has been ensured for the spandrel beam (as compared to the back-supporting beam) as it will be subjected to direct loads from the hydraulic jack.



**Fig. 4.** Strengthening of Spandrel Beam (a) Von Mises Stress Distribution, (b) Location of additional Stiffeners, and (c) Improved FEA Results.

### Prestress transfer

The transfer length is defined as the minimum distance along the bar from the end of the member over which the strain in the bar is less than 95% of the average maximum strain in the bar is known as 95% absolute maximum strain in the strand (AMSS) method. Another method typically known as 95% absolute maximum strain in the concrete (AMSC), is similar to AMSS method. However, the strains in the AMSC method are measured along the concrete surface at the level of the prestressing bar. Both the above-mentioned methodologies are based on a subjective assessment of the points belonging to the constant average strain plateau and considers the shear lag affects by reducing the peak strain value by 5% [33].

In the present study, the transfer length of the BFRP bar prestressed concrete beam specimens has been first predicted by plotting the 95% AMSS method (**Fig. 5(a)**). The transfer length has been found to be 190mm or  $24d_b$  (where,  $d_b$  is the diameter of the bar). The predicted transfer length is significantly lower than the transfer length for steel strands which is typically equal to  $50d_b$ . This is considered as an advantage over the conventional steel prestressing strands since a shorter transfer length would result in economical design of the BFRP prestressed concrete members.

It is difficult to obtain the transfer length in PC members using 95% AMSS since the strain gauges installed

on the bar can give inaccurate results due to several reasons. Firstly, the relative displacement between the bar and concrete results in debonding of the strain gauges mounted on the bar. Secondly, the presence of the strain gauges on the bar may affect the local bond stresses between the BFRP bar and the concrete resulting in inaccurate estimation of the transfer length. Hence, the strain gauges installed on BFRP bars in PC members are ineffective in measuring the transfer length using 95% AMSS along the pretensioned BFRP in practice.

Measurement of the strains on the concrete surface at the level of the prestressing element has proved to be the most reliable technique to measure the transfer length for PC members. The FEA results for concrete stress profile at the end of each analysis step of the present study are shown in **Fig. 5(b)**. The several kinks observed in the concrete stress profile is due to the development of plastic strains in concrete in the vicinity of the prestressing element over the transfer length region. Similar observation has been reported in previous studies by Martin *et. al.*, [34,35]. The transfer length has been predicted by averaging the concrete stress data and measuring the distance from the end of the concrete beam to the section of 95% AMSC. The transfer length obtained through this method has been found to be 210 mm ( $26d_b$ ) in lieu of 190 mm ( $24d_b$ ) observed using the 95% AMSS method. This observation is quite close to the experimental results reported by Crossett *et. al.*, [36] in which a transfer length for 12 mm BFRP bar was observed to be between 300 mm – 600 mm ( $25d_b$  to  $50d_b$ ) with the usage of 95% AMSC technique. However, it is to be noted that the transfer length is also dependent on several other factors such as type of tendon, concrete strength, concrete cover, bond condition, type of release, strand surface condition and strand slippage [33].

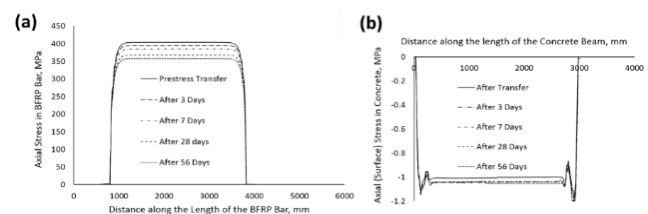


**Fig. 5.** Variation of Stress Profile, (a) along BFRP Bar, and (b) along Concrete Surface.

A comparison of the transfer length results obtained from the 95% AMSS and the 95% AMSC method is shown in **Table 2**. It has been observed that the transfer lengths obtained by directly measuring the strains on the BFRP bar during prestress transfer and by measuring the strains on the concrete surface at the bar location differ by less than 10% for 8 mm BFRP bars with an initial prestress of 400 MPa ( $0.40f_{pu}$ ). Thus, the present study shows that reasonably accurate transfer length can be measured using the 95% AMSC method by installing strain gauges on the concrete surface during experimental investigations of transfer lengths.

### End slip

The difference in concrete strains between the prestressing bar and the surrounding concrete over the transfer length region creates a relative slippage between the bar and concrete and is commonly known as end slips.

**Table 2.** Transfer Length and End Slip Results.

Step	Time (Days)	Prestress (MPa)	Transfer Length (mm)		End Slip (mm)
			95% of AMSS	95% of AMSC	
At Transfer	0	403.97			0.313
	3	395.48			0.272
Shrinkage and Creep	7	384.62	190	210	0.265
	28	367.56	(24d <sub>b</sub> )	(26d <sub>b</sub> )	0.249
	56	357.99			0.242

It is necessary to minimize these end slips since they significantly affect the transfer length and are majorly governed by the bond properties, level of reinforcement confinement and the initial prestress level. The end slips have been obtained directly from the FE model as the relative movement between the BFRP bar and concrete at the end of each step and are reported in **Table 2**. The end slips at the end of prestressing step have been found to be 0.313 mm indicating a good bond condition between the BFRP bar and concrete. The slips have been observed to reduce gradually in subsequent steps. This is primarily due to the increase in shrinkage and creep strain of concrete due to the time dependent parameters.

### Time dependent results

The increase in the concrete strains due to shrinkage and creep, results in the reduction of effective prestress of the bar. A total stress loss of approximately 46 MPa after prestress release has been observed at the end of 6<sup>th</sup> step (i.e., 56 days after prestress transfer). Note that the relaxation loss of BFRP bars have been neglected in the present simulation due to the insufficient data available on the long-term behavior of the BFRP bars utilized in the present study. Therefore, the actual loss in the experiment may be slightly higher than the FE prediction. The transfer length determined from the changed strain profiles of concrete and bar indicates that there is no significant change in the transfer length after the application of the prestressing force on the concrete beam. This observation could be due to the smaller dimension of the concrete member selected for the present study which is generally suitable for laboratory experiments.

### Concrete cracking

The kinks observed in the stress profile of concrete (shown in **Fig. 5(b)**) are attributed to the concrete cracking over the transfer length region. The plastic strains observed in the concrete beam adjacent to the bar reflect the development of cracks in the concrete beam during prestress transfer. The magnitude of these plastic strain decreases towards the center of the beam which indicates that its magnitude is

inversely proportional to the distance from the free end of the beam as shown in **Fig. 6**.

In order to control the stress concentration at the end of the pretensioned members and avoid cracking, several researchers deliberately debonded selected bars with concrete at and near the anchorage zones. However, the present study plans to release the prestress without debonding the bars for the better prediction of the state of stress and the nature of damage in the critical regions of concrete beams pretensioned with BFRP bars. This is necessary for taking effective steps towards controlling such cracks during prestress transfer.

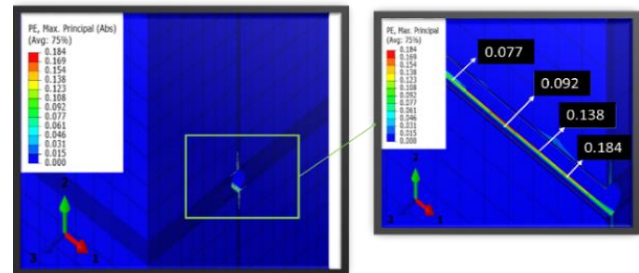


**Fig. 6.** Plastic Strains in the Concrete Beam after Prestress Transfer.

### Conclusion

The concern for durability and prolonged service life of concrete structures using FRP as prestressing element is rapidly gaining its significance with the ACI Committee releasing a report ACI 440R.04 [3] for the use of FRP for prestressing applications. However, the paucity of sufficient quantitative design data for the use of BFRP as prestressing strand has resulted into its elimination from the ACI report. In this paper, a design criterion for a test setup has been discussed to cast and prestress concrete beams using BFRP bars as prestressing element. The FE results depicted that the transfer length of the BFRP bars is approximately between 24d<sub>b</sub> to 26 d<sub>b</sub>. The results from time dependent FEA did not show significant increase in transfer length. Significant plastic strain formation in the concrete beam in the bar vicinity indicate concrete cracking over the transfer length region during prestress transfer. The present FEA investigation of the test setup points towards interesting observations that need to be corroborated through the actual experimental research. Thus, the test setup will be fabricated in the laboratory to perform experimental studies on concrete members prestressed using BFRP bars after the successful validation of the proof of concept of the design and the operation of the test setup using FE investigation. The results from the FEA model presented in the present study will be appropriately compared with the results obtained from the experimental investigation.

### Acknowledgements

The author of this work would like to acknowledge the Indian Institute of technology, Bombay for providing the high-computational facility requisite to perform the nonlinear analysis.

**Conflicts of interest**

There are no conflicts to declare.

**Keywords**

Basalt Fibre Reinforced Polymer, Finite Element Analysis, Prestressed Concrete and Transfer Length.

Received: 30 March 2021

Revised: 19 May 2021

Accepted: 29 May 2021

**References**

- Colajanni, P.; Recupero, A.; Ricciardi, G.; Spinella, N.; *Int. J. Struct. Integr.*, **2016**, *7*, 181.
- Poston, R. W.; West, J. S.; Investigation of the Charlotte Motor Speedway Bridge Collapse, *Int. Proc. Struct. Congr. Expo.*, **2005**.
- ACI 440.4R, Prestressing Concrete Structures with FRP Tendons, *ACI Comm.*, **2004**, pp.1-35.
- PCI Committee on Prestress Losses, *PCI J.*, **1975**, *18*, 43.
- Singh, S.; Kumar, P.; Jain, S. K.; *Adv. Mater. Lett.*, **2013**, *4*, 567.
- Kulkarni, V.; Jaiswal, M.; Ramtekkar, G.; *Adv. Mater. Lett.*, **2020**, *11*, 20091553.
- Dolan, C. W.; Nanni, A.; *Adv. Cem. Based Mater.*, **1994**, *1*, 185.
- Nanni, A.; Tanigaki, M.; *ACI Struct. J.*, **1992**, *89*, 433.
- Ehsani, M. R.; Saadatmanesh, H.; Nelson, C. T.; *PCI J.*, **1997**, *42*, 76.
- Scruggs, A. M.; Henderson, K.; Hsiao, K.; "Characterization of Electrical Conductivity of a Carbon Fiber Reinforced Plastic Laminate Reinforced with Z-Aligned Carbon Nanofibers," *Proc. Compos. Adv. Mater. Expo (CAMX 2016)*, **2016**, no. 11, Anaheim, CA, pp. 26-29.
- Li, J.; Zhao, Z.; "Study on Mechanical Properties of Basalt Fiber Reinforced Concrete," 5th Int. Conf. Environ. Mater. Chem. Power Electron. (EMCPE 2016), **2016**, no.2, pp.583-587.
- Abed, F.; Al-Mimar, M.; Ahmed, S.; *Compos. Part C*, **2021**, *4*, 100107.
- Abed, F.; Oucif, C.; Awera, Y.; Mhanna, H.; Alkhraisha, H.; *Def. Technol.*, **2021**, *17*, 1.
- Abed, F.; Mehaini, Z.; Oucif, C.; Abdul-Katif, A.; Baleh, R.; *Compos. Part C*, **2021**, *2*, 100034.
- Alkhraisha, H.; Mhanna, H.; Abed, F.; "FE Modeling of RC Beams Reinforced in Flexure with BFRP Bars Exposed to Harsh Conditions," *Sustain. Issues Infrastruct. Eng.*, **2021**, vol. book series, pp.3-13.
- Rifai, M.; El-Hassan, H.; El-Maaddawy, T.; Abed, F.; *Constr. Build. Mater.*, **2020**, *243*, 118258.
- Wu, Z.; Wang, X.; Wu, G.; "Basalt FRP Composite as Reinforcements in Infrastructure," in *Annual International Conference on Composites/nano Engineering*, **2009**, pp. 4-11.
- Mander, J. B.; Priestley, M. J. N.; Park, R.; *J. Struct. Eng.*, **1988**, *144*.
- Motwani, P.; Perogamvros, N.; Taylor, S.; Sonebi, M.; Laskar, A.; "Study on Anchor Efficiency and Stress Relaxation of BFRP Bars using Digital Image Correlation and FBG Sensing Technology," *Proc. Fibre Reinf. Polym. Reinf. Concr.*, **2019**, vol. 14.
- ASTM A276 / A276M-17, "Standard Specification for Stainless Steel Bars and Shapes," ASTM International, West Conshohocken, Pennsylvania, United States, **2017**.
- Yun, X.; Gardner, L.; *J. Constr. Steel Res.*, **2017**, *133*, 36.
- Lago, P. D.; Taylor, S.; Deegan, P.; Ferrara, L.; Sonebi, M.; Crosset, P.; *Compos. Part B Eng.*, **2017**, *128*, 120.
- Sólyom, S.; "Report on Bond Test Results of Galen Composites FRP Bars," Budapest University of Technology and Economics, Budapest, Hungary, **2017**.
- Lupasteanu, V.; Taranu, N.; Popoaei, S.; "Theoretical Strength Properties of Unidirectional Reinforced Fiber Reinforced Polymer Composites," *Bull. Polytech. Inst. Jassy, Constr. Archit. Sect.*, **2013**, no. 6, pp. 83-98.
- Chamis, C.; *J. Compos. Technol.*, **1989**, *11*, 3.
- Elgabbas, F.; Ahmed, E.; Benmokrane, B.; "Basalt FRP Reinforcing Bars for Concrete Structures," 4th Asia-Pacific Conf. FRP Struct. (APFIS 2013), **2013**, Vol. 440, no. 12, pp. 11-13.
- Laskar, A.; Motwani, P.; Khan, N.; "System and Method for Producing Prestressed Concrete Composite Beam Using Fibre Reinforced Polymer Bar," Indian Patent Office (IPO), Patent-WO2020075195, **2020**.
- Eurocode-2, "Design of Concrete Structures - Part 1-1: General Rules and Rules for Buildings," *Eur. Stand.*, **1992**.
- Motwani, P.; Laskar, A.; *Structures*, **2019**, *20*, 676.
- AASHTO LRFDF, "AASHTO LRFDF Bridge Design Specifications," Am. Assoc. State Highw. Transp. Off., **2007**.
- Yuan, J.; Hadi, M.; *Mater. Struct.*, **2018**, *51*, 31.
- Motwani, P.; Laskar, A.; "Finite Element Analysis of Bond Slip Behavior in Pretensioned Bridge Girder," *Prestress. Concr. Instiute Conv.*, Denver, Colorado, **2018**.
- Buckner, C. D.; "An Analysis of Transfer and Development lengths for Pretensioned Concrete Structure," U.S. Dept. of Transportation, Lexington, **1994**.

- Martin, J.; Russell, T.; Bruce, N.; *PCI J.*, **1993**, *38*, 34.
- Andrawes, B.; Shin, M.; Pozolo, A.; "Transfer and Development Length of Prestressing Tendons in Full-Scale AASHTO Prestressed Concrete Girders using Self-Consolidating Concrete," University of Illinois at Urbana-Champaign, Champaign, IL, **2009**.
- Crosset, P.; Taylor, S.; Sonebi, M.; Robinson, D.; Garcia-Taengua, E.; "Monitoring the Transfer Length of Prestressed BFRP SCC Beams," 7th Int. Conf. Struct. Heal. Monit. Intell. Infrastruct. (ISHMII7), Torino, Italy., **2015**.

**Author's biography**



**Prashant Motwani** holds Bachelors and Master's degrees in Civil/Structural Engineering. He is currently in the fifth year of his PhD and his research interests centre around replacement of steel pre-stressing strand with fibre reinforced polymer bars in pre-stressed concrete structures.

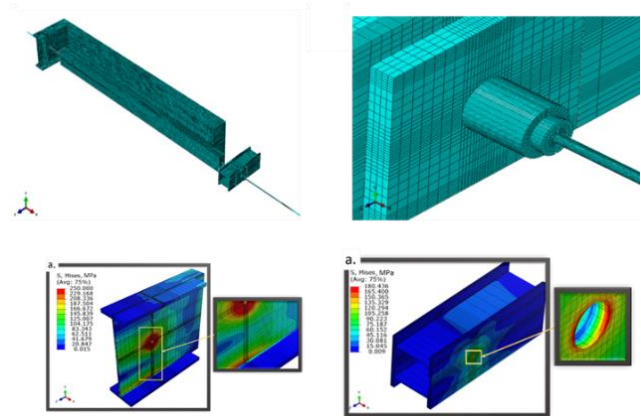


**Shruti Dhruw** holds a Master's degree in Structural Engineering from Indian Institute of Technology, Bombay. Her research work is primarily focussed upon the finite element modelling of mechanical anchors and parametric studies on BFRP prestressed beams. She is currently working as an Assistant Engineer in Chhattisgarh State Power Corporation.



**Dr. Arghadeep Laskar** is Associate Professor in the Civil Engineering Department of IIT Bombay in India since 2014. Prior to that he worked as a Structural Engineer in the offshore industry in Houston for five years after completing his PhD at University of Houston. His primary research interests are in the area of sustainability and design improvement through large-scale tests and FEA simulation of concrete structures. He is a licensed professional engineer in the state of Texas (USA) and serves as the reviewer for various technical and scientific journals.

**Graphical abstract**



A robust 3D nonlinear FE model of a test-frame to fabricate and prestress concrete beams with BFRP bars has been developed. The configuration details of the test-frame have been studied and the effects of the size and orientation of the sections and location of the stiffener plates on the overall performance of the test setup have been investigated. The transfer-stage parameters for BFRP prestressed concrete beams have been estimated using the FE model.